



저작자표시-비영리-변경금지 2.0 대한민국

이용자는 아래의 조건을 따르는 경우에 한하여 자유롭게

- 이 저작물을 복제, 배포, 전송, 전시, 공연 및 방송할 수 있습니다.

다음과 같은 조건을 따라야 합니다:



저작자표시. 귀하는 원저작자를 표시하여야 합니다.



비영리. 귀하는 이 저작물을 영리 목적으로 이용할 수 없습니다.



변경금지. 귀하는 이 저작물을 개작, 변형 또는 가공할 수 없습니다.

- 귀하는, 이 저작물의 재이용이나 배포의 경우, 이 저작물에 적용된 이용허락조건을 명확하게 나타내어야 합니다.
- 저작권자로부터 별도의 허가를 받으면 이러한 조건들은 적용되지 않습니다.

저작권법에 따른 이용자의 권리는 위의 내용에 의하여 영향을 받지 않습니다.

이것은 [이용허락규약\(Legal Code\)](#)을 이해하기 쉽게 요약한 것입니다.

[Disclaimer](#)

M.S. THESIS

Ashkin-Teller Model on Scale-Free Networks

척도 없는 네트워크에서의 에쉬킨-텔러 모형

FEBRUARY 2014

Department of Physics and Astronomy
College of Natural Sciences
Seoul National University

Siho Jang

Ashkin-Teller Model on Scale-Free Networks

척도 없는 네트워크에서의 에쉬킨-텔러 모형

지도교수 강병남

이 논문을 이학석사 학위논문으로 제출함

2013년 11월

서울대학교 대학원

물리·천문학부

장시호

장시호의 석사 학위논문을 인준함

2013년 12월

위원장	유재준	(인)
부위원장	강병남	(인)
위원	박철환	(인)

Abstract

Ashkin-Teller Model on Scale-Free Networks

장시호 (Siho Jang)

Department of Physics and Astronomy

The Graduate School

Seoul National University

The investigation of various spin models on complex networks has played a crucial role in the comprehension of collective behavior in natural phenomena. In particular, the Ising and the Potts model on networks have received attention in the last decade for such purposes. Recently, multiplex networks have been actively studied in detail, because many real-world networks are networks of networks. Despite these facts, only a few spin models that incorporate interactions between nodes on inter- and intra-networks have been studied yet.

In this paper, we study the Ashkin-Teller (AT) model on scale-free random networks. In the AT model, spins on each site are of two types, and two spins of each type at the nearest neighbors interact with coupling strength J_2 , and four spins of both types at the nearest neighbors interact with coupling strength J_4 . In other words, J_2 and J_4 correspond to the interaction constants of the spins on the intra- and the inter-network, respectively.

As was seen in the mean-field approximation, various phases emerge depending on the ratio $x = J_4/J_2$. Some examples of such phases are the paramagnetic phase, ferromagnetic phase, anti-ferromagnetic phase, the Baxter phase, and the sigma phase. We obtain the phase diagram on scale-free networks. While the

phase transition between paramagnetic phase and the Baxter phase is discontinuous in the standard mean-field solution, it can be continuous depending on the degree exponent on scale-free network. In spirit of the Landau theory, we focus on this tricritical point that divides the phase space into regimes of the first- and second-order phase transition. Then we obtain the critical degree exponent as a function of x using the analytical approach. For positive x , we can thus determine the type of order of the phase transition on scale-free networks in terms of x and the degree exponent.

In addition, we perform Monte Carlo simulation using the Metropolis algorithm to sketch the schematic phase diagram for $x < 0$. Besides the diagram, a variety of thermodynamic quantities, such as magnetizations, heat capacity, susceptibility, the Binder cumulant, can come along for the ride. In this regime, anomalous behavior due to frustration can be observed.

Finally, we examine the analytic and simulation results, and discuss the implications of the difference in the mean-field level between the phase diagrams of scale-free networks and homogeneous space.

Keywords: Ashkin-Teller model, Scale-free networks, Continuous phase transition, Discontinuous phase transition, Critical degree exponents, Tricritical point, Monte-Carlo simulation, Metropolis algorithm

Student Number: 2012-22512

Contents

Abstract	i
Contents	iii
List of Figures	v
Chapter 1 Introduction	1
Chapter 2 The Ashkin-Teller Model	4
Chapter 3 Mean-Field Approximation	9
3.1 Partition function and mean field hamiltonian	9
3.2 Mean field free energy	11
Chapter 4 The AT Model on Uncorrelated Scale-Free Networks	14
4.1 Mean field free energy in the infinite network limit	15
4.2 Equations of state	16
4.3 Example 1 : the Ising model	19
4.4 Example 2 : the 4-state Potts model	19
4.5 Critical degree exponent of the AT model	21
4.6 Brief simulation results	25

Chapter 5 Conclusion	29
요약	35

List of Figures

Figure 2.1	The schematic drawing of the isotropic AT model on multiplex networks. This network consists of two layers which have exactly same structure. Each intra-network is the uncorrelated scale-free network, while inter-network has one-to-one connections. Spin σ and s lie on the nodes of each network, respectively. The interaction strength between same type of spins is given by J_2 . J_4 represent the four-spin interaction in two different layers. We note that the ratio of coupling strengths J_4/J_2 determines the nature of phase transition.	8
------------	---	---

Figure 4.1	The phase diagram of the isotropic AT model on uncorrelated scale-free networks. λ is the degree exponent and x is the ratio of the coupling strengths (J_4/J_2). Blue points indicate the critical degree exponents obtained by numerical calculation. The regime over the line belongs to the first-order phase transition, while that below belongs to the second-order phase transition. The Potts point is at $x = 1$, which is equivalent to universality class of the 4-state Potts model. The Potts point is the minimum of λ . This implies that system on the Potts point($x = 1$) need stronger hubs to change type of ordering from first-order to second-order transition.	25
Figure 4.2	Magnetizations of the AT model on scale-free networks depending on temperature(T , $k_B = 1$) with $\lambda = 3.6$, N (the number of nodes)= 50000, and $x = 1.0$	27
Figure 4.3	Magnetizations of the AT model on scale-free networks depending on temperature(T , $k_B = 1$) with $\lambda = 3.6$, N (the number of nodes)= 50000, and $x = 0.0$	27
Figure 4.4	Magnetizations of the AT model on scale-free networks depending on temperature(T , $k_B = 1$) with $\lambda = 3.6$, N (the number of nodes)= 50000, and $x = -0.5$	27
Figure 4.5	Magnetizations of the AT model on scale-free networks depending on temperature(T , $k_B = 1$) with $\lambda = 3.6$, N (the number of nodes)= 50000, and $x = -0.9$	27
Figure 4.6	Magnetizations of the AT model on scale-free networks depending on temperature(T , $k_B = 1$) with $\lambda = 3.6$, N (the number of nodes)= 50000, and $x = -1.0$	28

Figure 4.7	Magnetizations of the AT model on scale-free networks depending on temperature(T , $k_B = 1$) with $\lambda = 3.6$, N (the number of nodes)= 50000, and $x = -1.1$	28
Figure 4.8	Magnetizations of the AT model on scale-free networks depending on temperature(T , $k_B = 1$) with $\lambda = 3.6$, N (the number of nodes)= 50000, and $x = -1.5$	28
Figure 4.9	Magnetizations of the AT model on scale-free networks depending on temperature(T , $k_B = 1$) with $\lambda = 3.6$, N (the number of nodes)= 50000, and $x = -2.0$	28

Chapter 1

Introduction

Recently, multiplex networks have been intensively studied in detail, because many real-world networks can be seen as networks of networks. This means that real-world systems are coupled interacting networks. various infrastructure, such as, power station, transportation, communications networks, water supply, Internet, etc, are tangled up. Therefore, a careful study of interdependent networks will be fruitful.

In 2010, Sergey V. Buldyrev *et al.* studied 'catastrophic cascade of failures in interdependent networks' motivated by the electrical blackout that happened on 28 September 2003 in Italy [1]. They mapped the power network and the Internet into an interdependent network, and demonstrated that the iterative cascade of failures in this network is a first-order phase transition from the view of percolation. Moreover, Krzysztof Suchecki and Janusz A. Hołyst investigated the Ising model on two sparsely connected Barabási-Albert(BA) networks [2–4], in the mean-field dynamics. The two BA networks are connected by the preferential probability of each node in the network. In such model, they discovered a

bistable-monostable phase transition, and observed a discontinuous jump of the magnetization [5]. These results significantly imply that a discontinuous phase transition can occur due to the properties determined by the structure of the intra-networks and their interactions.

In these backgrounds, we set out to study the spin model on multiplex networks, and apply to this the AT model [6]. We simplify this network to a two-layer network where each intra-network is an uncorrelated scale-free network and has exactly the same structure (see Fig. 2.1). Each node has a one-to-one connection with its mirror node in the other intra-network. Let us call the spins of the nodes in the upper layer σ , and those in the lower layer s . Each spin interacts with its intra-network neighbors with a coupling strength $J_{2,s}$ or $J_{2,\sigma}$ depending on its own spin. On the inter-network, the spins are coupled by a four-spin interaction J_4 . Here we will only consider the isotropic AT model: $J_2 = J_{2,s} = J_{2,\sigma}$. While the phase transition between paramagnetic phase and the Baxter phase is discontinuous in the mean-field level [7], it can be continuous depending on the degree exponent of scale-free networks. In other words, there exists a critical degree exponent that divides the phase space into regimes of the first- and second-order phase transition. We will show that the value of the critical degree exponent depends on the ratio $\frac{J_4}{J_2}$. Clearly, the discontinuous phase transition can occur depending on the structure of the network and the strength of the interaction of the inter-network.

In next chapter, we introduce the historical background of the AT model, along with some of works done relating to this topic. We study two well-known examples, the two-dimensional square lattice and a Cayley tree case. chapter 3 is devoted to finding the standard mean-field free energy for the AT model. Then in chapter 4, we analytically calculate the annealed mean-field free energy and the self-consistency equations (or equations of state) for the

isotropic AT model on uncorrelated scale-free networks. In addition, we discuss the anticipated type of the phase diagram with numerical results along with the Monte-Carlo simulation results. Finally in chapter 5, we will conclude the paper with a brief summary and some discussion of the possible future works.

Chapter 2

The Ashkin-Teller Model

J. Ashkin and E. Teller considered “a two-dimensional square net consisting of four kinds of atoms supposing that only nearest neighbors interact and that there are only two distinct potential energies of interaction, one between like and one between unlike atoms” [6]. Their model, which is considered as a four component system, is relevant to the generalization of the Ising model. Each site of two-dimensional square net is occupied with one of the four kinds of atoms, namely, A, B, C, and D. The interaction energies between neighboring atoms are defined to be: ϵ_0 for $A-A$, $B-B$, $C-C$, $D-D$, ϵ_1 for $A-B$, $C-D$, ϵ_2 for $A-C$, $B-D$, and ϵ_3 for $A-D$, $B-C$. Using the duality from Kramers-Wannier(1941) and the reciprocity relation of Onsager, they obtained the partition function and conjectured the location of the Curie temperature.

C. Fan expressed this model in terms of the Ising spin [8]. Each lattice site i has two spins: s_i and σ_i . He represented the four atoms A, B, C, and D by the four possible spin configurations (s_i, σ_i) : $A \rightarrow (+, +)$, $B \rightarrow (+, -)$, $C \rightarrow$

$(-, +)$, and $D \rightarrow (-, -)$. Then, the Hamiltonian for the system is given by

$$\mathcal{H} = \sum_{i,j} [-J_{2,s} s_i s_j - J_{2,\sigma} \sigma_i \sigma_j - J_4 s_i \sigma_i s_j \sigma_j - J_0], \quad (2.1)$$

where

$$\begin{aligned} -J &= (\epsilon_0 + \epsilon_1 - \epsilon_2 - \epsilon_3)/4 \\ -J' &= (\epsilon_0 + \epsilon_2 - \epsilon_3 - \epsilon_1)/4 \\ -J_4 &= (\epsilon_0 + \epsilon_3 - \epsilon_1 - \epsilon_2)/4 \\ -J_0 &= (\epsilon_0 + \epsilon_1 + \epsilon_2 + \epsilon_3)/4. \end{aligned} \quad (2.2)$$

Then, the partition function is

$$Z_{\text{AT}} = \sum_s \sum_{\sigma} \exp [-\beta H], \quad (2.3)$$

where $\beta = \frac{1}{k_B T}$, with k_B being the Boltzmann constant, T being the temperature. The summations run over all possible values of each spin. The constant term J_0 does not have any effect on the various thermodynamic quantities and can be neglected. The Hamiltonian and the partition function without J_0 is widely known. Therefore, the AT model may be considered as two superposed Ising models with four-spin interaction.

In two-dimensional lattice, Wegner showed the AT model's equivalence to the staggered eight-vertex model [9]. Baxter solved the isotropic AT model by mapping it into the staggered eight-vertex(8V) model which in turn reduces to the six-vertex(6V) model in zero external field. However, the general AT model including the condition $J_{2,s} \neq J_{2,\sigma}$ remains unsolved. The isotropic AT model in a square lattice has been investigated extensively and its structure of the complete phase diagram has been obtained [7], using the Monte Carlo simulation [10–12], an experimental technique [13], and theoretical methods including renormalization group approach [14–17].

Furthermore, the phase diagram for the isotropic AT model in a cubic lattice has been studied by means of mean field theory, series data and Monte Carlo analysis [7]. Surprisingly, the phase diagram of the isotropic AT model has a very rich phase and consists of a various critical line, while the phase diagram in three-dimension is quite different from that in two-dimension. Depending on the ratio of coupling strengths $x = J_4/J_2$ and temperature T , the phase consists of five kinds of phase such as, (a) paramagnetic phase *Para* which is fully disordered $\langle s \rangle = 0$, $\langle \sigma \rangle = 0$, $\langle s\sigma \rangle = 0$ ($\langle \cdots \rangle$ denotes the thermal average), (b) the *Baxter* phase which is fully ordered $\langle s \rangle = \pm \langle \sigma \rangle \neq 0$, $\langle s\sigma \rangle \neq 0$, (c) the ferromagnetic phase $\langle s\sigma \rangle$ which is partially ordered $\langle s \rangle = 0$, $\langle \sigma \rangle = 0$, $\langle s\sigma \rangle \neq 0$ (d) the ferromagnetic phase $\langle s \rangle$ which is partially ordered $\langle s \rangle \neq 0$, $\langle \sigma \rangle = 0$, $\langle s\sigma \rangle = 0$. Under the permutations $s \leftrightarrow \sigma$, the symmetry of the AT model keeps invariant. (e) the anti-ferromagnetic phase $\langle s\sigma \rangle_{\text{AF}}$ in which the phase $\langle s \rangle$ and $\langle \sigma \rangle$ are disordered, but $s\sigma$ is ordered anti-ferro-magnetically. It is noticed that $\langle s \rangle$ phase appears for $-1 \lesssim x \lesssim -0.5$, and $\langle s \rangle_{\text{AF}}$ appears for $x \lesssim -1$ in mean field level. And they showed that the first-order phase transition can be occurred in three dimensions. But it is hard to distinguish the weakly first-order from the second-order behavior in the vicinity of tricritical point. Arnold and Zhang obtained more accurate results for very weakly first-order transitions in three dimensions, by means of Monte Carlo simulations [18]. Moreover, Musial *et al.* investigated more accurately the tricritical behavior for the isotropic AT model in three dimensions, using the Monte Carlo simulation. They analyzed the fourth-order-cumulant, the Binder cumulant, and the Challa-like cumulant, using the finite-size-scaling analysis and the universality hypothesis. From these results, they estimated the location of tricritical points [19, 20].

In other lattices, the competition between two-coupling strength J and four-coupling strength J_4 lead to distinct phase diagrams according the topology of

structure. For example, the isotropic AT model phase diagram on the Cayley tree of finite coordination z was obtained by solving the recursion relations and finding the fixed point [21]. this results reveals distinct topologies depending on z and the ratio of x . And the distinct phase diagram for the isotropic and anisotropic AT model on Bethe Lattice has been studied, restricted to the case of ferromagnetic interaction, i.e., for $x > 0$ [22]. They showed that the phase diagrams for the anisotropic AT model in the case of $J_{2,s} > J_{2,\sigma}$ are equivalent with those in the case of $J_{2,s} < J_{2,\sigma}$, only replacing the $\langle s \rangle$ phase by the $\langle \sigma \rangle$ phase. Thus, even in the anisotropic AT model, the symmetry keeps invariant under the permutation $J_{2,s} \leftrightarrow J_{2,\sigma}$.

Now, we deal with the AT model on uncorrelated scale-free networks (see in Fig. 2.1). Networks which are more complicated connectivities than regular lattices, have been researched in detail, recently. We consider the networks topology and interactions between linked nodes, and investigate the ordering phenomenon on complex networks, if spins of the AT model type are put onto the nodes of the network. We solve the isotropic AT model on such networks, applying the mean field approximation and considering the weight effect induced from the heterogeneous links what each nodes possess. And we perform the Monte-Carlo simulations to obtain some results which cannot covered by theoretical method.

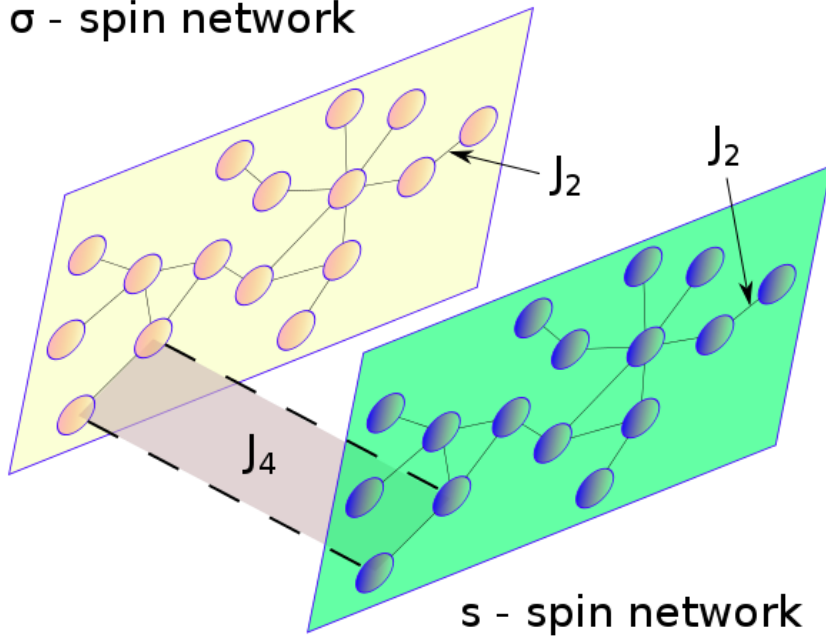


Figure 2.1 The schematic drawing of the isotropic AT model on multiplex networks. This network consists of two layers which have exactly same structure. Each intra-network is the uncorrelated scale-free network, while inter-network has one-to-one connections. Spin σ and s lie on the nodes of each network, respectively. The interaction strength between same type of spins is given by J_2 . J_4 represent the four-spin interaction in two different layers. We note that the ratio of coupling strengths J_4/J_2 determines the nature of phase transition.

Chapter 3

Mean-Field Approximation

We begin by introducing the Hamiltonian of the AT model.

$$\begin{aligned}\mathcal{H} = & -J_2 \sum_{\langle i,j \rangle} s_i s_j - J_2 \sum_{\langle i,j \rangle} \sigma_i \sigma_j - J_4 \sum_{\langle i,j \rangle} s_i \sigma_i s_j \sigma_j \\ & - H_s \sum_i s_i - H_\sigma \sum_i \sigma_i - H_{s\sigma} \sum_i s_i \sigma_i ,\end{aligned}\tag{3.1}$$

where i and $\langle i, j \rangle$ run over all of the nodes and links of a given network, respectively.

3.1 Partition function and mean field hamiltonian

In statistical physics, the partition function is given by

$$Z = \sum_{\{s_i, \sigma_i\}} e^{-\beta \mathcal{H}}.\tag{3.2}$$

where the summation $\sum_{\{s_i, \sigma_i\}}$ is over the up-spin and down-spin of each of the spins on the network which are respectively the values $+1$ and -1 .

For convenience, we will deal with the reduced Hamiltonian, which is the Hamiltonian multiplied by $-\beta$

$$\begin{aligned}
-\beta\mathcal{H} = & K_2 \sum_{\langle i,j \rangle} s_i s_j + K_2 \sum_{\langle i,j \rangle} \sigma_i \sigma_j + K_4 \sum_{\langle i,j \rangle} s_i \sigma_i s_j \sigma_j \\
& + h_s \sum_i s_i + h_\sigma \sum_i \sigma_i + h_{s\sigma} \sum_i s_i \sigma_i .
\end{aligned} \tag{3.3}$$

Using the standard mean field approximation, we define order parameters which are the thermodynamic spin averages of each node:

$$m_s^i = \frac{\sum_{\{s_i, \sigma_i\}} (s_i e^{-\beta\mathcal{H}})}{Z} \tag{3.4}$$

$$m_\sigma^i = \frac{\sum_{\{s_i, \sigma_i\}} (\sigma_i e^{-\beta\mathcal{H}})}{Z} \tag{3.5}$$

$$m_{s\sigma}^i = \frac{\sum_{\{s_i, \sigma_i\}} (s \sigma_i e^{-\beta\mathcal{H}})}{Z}. \tag{3.6}$$

Since we can approximate the effects on each spin of other spins by introducing an effective field, let us expand each spin about the local order parameter:

$$s_i = m_s^i + \delta m_s^i + \dots \tag{3.7}$$

$$\sigma_i = m_\sigma^i + \delta m_\sigma^i + \dots \tag{3.8}$$

$$s\sigma_i = m_{s\sigma}^i + \delta m_{s\sigma}^i + \dots \tag{3.9}$$

After neglecting the contributions of second- and higher-order terms of each spin, substitution of Eq. (3.7), Eq. (3.8), and Eq. (3.9) into the reduced

Hamiltonian gives

$$\begin{aligned}
-\beta\mathcal{H}_{\text{mf}} &\simeq +K_2 \sum_{\langle i,j \rangle} \left(m_s^i m_s^j + m_s^i \delta m_s^j + \delta m_s^i m_s^j + m_\sigma^i m_\sigma^j + m_\sigma^i \delta m_\sigma^j + \delta m_\sigma^i m_\sigma^j \right) \\
&\quad + K_4 \sum_{\langle i,j \rangle} \left(m_{s\sigma}^i m_{s\sigma}^j + m_{s\sigma}^i \delta m_{s\sigma}^j + \delta m_{s\sigma}^i m_{s\sigma}^j \right) \\
&\quad + h_s \sum_i \left(m_s^i + \delta m_s^i \right) + h_\sigma \sum_i \left(m_\sigma^i + \delta m_\sigma^i \right) + h_{s\sigma} \sum_i \left(m_{s\sigma}^i + \delta m_{s\sigma}^i \right) \\
&\simeq +K_2 \sum_{\langle i,j \rangle} \left[m_s^i m_s^j + m_\sigma^i m_\sigma^j + 2m_s^j \left(s_i - m_s^i \right) + 2m_\sigma^j \left(\sigma_i - m_\sigma^i \right) \right] \\
&\quad + K_4 \sum_{\langle i,j \rangle} \left[m_{s\sigma}^i m_{s\sigma}^j + 2m_{s\sigma}^j \left(s_i \sigma_i - m_{s\sigma}^i \right) \right] \\
&\quad + h_s \sum_i s_i + h_\sigma \sum_i \sigma_i + h_{s\sigma} \sum_i s_i \sigma_i \\
&\simeq -K_2 \sum_{\langle i,j \rangle} \left(m_s^i m_s^j + m_\sigma^i m_\sigma^j - 2m_s^j s_i - 2m_\sigma^j \sigma_i \right) \\
&\quad - K_4 \sum_{\langle i,j \rangle} \left(m_{s\sigma}^i m_{s\sigma}^j - 2m_{s\sigma}^j s_i \sigma_i \right) \\
&\quad + h_s \sum_i s_i + h_\sigma \sum_i \sigma_i + h_{s\sigma} \sum_i s_i \sigma_i
\end{aligned} \tag{3.10}$$

where the subscript mf denotes the use of the mean field approximation.

3.2 Mean field free energy

The free energy is

$$F = -k_B T \ln Z \simeq -k_B T \ln \left[\sum_{\{s_i, \sigma_i\}} \exp(-\beta\mathcal{H}_{\text{mf}}) \right] \tag{3.11}$$

By means of Eq. (3.10), we get the mean field free energy

$$\begin{aligned}
F_{\text{mf}} &\simeq -k_B T \ln \left[\sum_{\{s_i, \sigma_i\}} \exp \left(-K_2 \sum_{\langle i,j \rangle} \left(m_s^i m_s^j + m_\sigma^i m_\sigma^j \right) - K_4 \sum_{\langle i,j \rangle} m_{s\sigma}^i m_{s\sigma}^j \right) \right. \\
&\quad \left. \times \exp \left(K_2 \sum_{\langle i,j \rangle} \left(2m_s^j s_i + 2m_\sigma^j \sigma_i \right) + K_4 \sum_{\langle i,j \rangle} 2m_{s\sigma}^j s_i \sigma_i + \text{field part} \right) \right] \\
&\simeq -k_B T \ln \left[\exp \left(-K_2 \sum_{\langle i,j \rangle} \left(m_s^i m_s^j + m_\sigma^i m_\sigma^j \right) - K_4 \sum_{\langle i,j \rangle} m_{s\sigma}^i m_{s\sigma}^j \right) \right. \\
&\quad \left. \times \sum_{\{s_i, \sigma_i\}} \exp \left(K_2 \sum_{\langle i,j \rangle} \left(2m_s^j s_i + 2m_\sigma^j \sigma_i \right) + K_4 \sum_{\langle i,j \rangle} 2m_{s\sigma}^j s_i \sigma_i + \text{field part} \right) \right] \\
&\simeq -k_B T \ln \left[\exp \left(-K_2 \sum_{\langle i,j \rangle} \left(m_s^i m_s^j + m_\sigma^i m_\sigma^j \right) - K_4 \sum_{\langle i,j \rangle} m_{s\sigma}^i m_{s\sigma}^j \right) \right. \\
&\quad \left. \times \sum_{\{s_i, \sigma_i\}} \exp \left(K_2 \sum_i \sum_{j(i)} \left(m_s^j s_i + m_\sigma^j \sigma_i \right) + K_4 \sum_i \sum_{j(i)} m_{s\sigma}^j s_i \sigma_i + \text{field part} \right) \right] \\
&\simeq -k_B T \ln \left[\exp \left(-K_2 \sum_{\langle i,j \rangle} \left(m_s^i m_s^j + m_\sigma^i m_\sigma^j \right) - K_4 \sum_{\langle i,j \rangle} m_{s\sigma}^i m_{s\sigma}^j \right) \times \prod_i Z_i \right] , \\
&\hspace{25em} (3.12)
\end{aligned}$$

where the local partition function is defined by

$$Z_i = \sum_{\{s_i, \sigma_i\}} \exp \left(K_2 \sum_{j(i)} \left(m_s^j s_i + m_\sigma^j \sigma_i \right) + K_4 \sum_{j(i)} m_{s\sigma}^j s_i \sigma_i + h_s s_i + h_\sigma \sigma_i + h_{s\sigma} s_i \sigma_i \right) . \quad (3.13)$$

In Eq. (3.13), $j(i)$ is the set of all nearest-neighboring nodes of i .

The logarithm of Eq. (3.12) can be divided into sums.

$$\begin{aligned}
\beta F &\simeq -\ln \left[\exp \left(-K_2 \sum_{\langle i,j \rangle} \left(m_s^i m_s^j + m_\sigma^i m_\sigma^j \right) - K_4 \sum_{\langle i,j \rangle} m_{s\sigma}^i m_{s\sigma}^j \right) \right] - \sum_i \ln Z_i \\
&= -\sum_i \ln Z_i + K_2 \sum_{\langle i,j \rangle} m_s^i m_s^j + K_2 \sum_{\langle i,j \rangle} m_\sigma^i m_\sigma^j + K_4 \sum_{\langle i,j \rangle} m_{s\sigma}^i m_{s\sigma}^j.
\end{aligned} \tag{3.14}$$

And we readily obtained the local partition function Z_i after some calculations

$$\begin{aligned}
Z_i &= \sum_{\{s_i, \sigma_i\}} Z_i[s_i, \sigma_i] \\
&= Z_i[+, +] + Z_i[+, -] + Z_i[-, +] + Z_i[-, -] \\
&= 4 \left[\cosh \left(\sum_{j(i)} K_2 m_s^j + h_s \right) \cosh \left(\sum_{j(i)} K_2 m_\sigma^j + h_\sigma \right) \cosh \left(\sum_{j(i)} K_4 m_{s\sigma}^j + h_{s\sigma} \right) \right. \\
&\quad \left. + \sinh \left(\sum_{j(i)} K_2 m_s^j + h_s \right) \sinh \left(\sum_{j(i)} K_2 m_\sigma^j + h_\sigma \right) \sinh \left(\sum_{j(i)} K_4 m_{s\sigma}^j + h_{s\sigma} \right) \right].
\end{aligned} \tag{3.15}$$

The free energy Eq. (3.14) with this partition function consistent with that obtained by Ditzain *et al.* [7].

Chapter 4

The AT Model on Uncorrelated Scale-Free Networks

In the last decade, the Ising model on complex networks had been studied using the mean field calculations [3, 23, 24] which leads to a variety of approaches, including replica method [25], recurrence relations assuming tree-like structure [26], the steepest descent method [27].

Furthermore, the q -state Potts model had been similarly investigated by an effective medium Cayley-tree approach [28] and two mean-field approaches, one dealing with self-consistency equations [29], another analyzing the free energy in the viewpoint of the Landau theory [30]. To sum up, all three agree that the fat-tailed degree distribution increases the critical temperature and suppresses first-order phase transition.

Likewise, we can apply the above methods to the isotropic AT model on scale-free networks. Now, we will deal with the AT model using the annealed mean free energy and find the equation of state. Then we'll also estimate the critical degree exponent λ_c which is in the vicinity of the boundary between

first- and second-order phase transition, from the perspective of the Landau theory.

4.1 Mean field free energy in the infinite network limit

Complex networks have an intrinsic heterogeneous structure where different nodes possess different degrees. Thus we need to introduce a global order parameter related to the magnetization of nodes that is assigned to be the weighted sum of the local order parameters [29, 30]:

$$m = \frac{\sum_i k_i m_i}{\sum_i k_i} = \frac{\sum_i k_i m_i}{N \langle k \rangle} \quad (4.1)$$

where $\langle k \rangle = \frac{1}{N} \sum_{i=1}^N k_i$ is the mean degree.

For the same reason, we give the coupling constant the probability P_{ij} that the node i is connected to the node j to be

$$K_{ij} = K P_{ij} = K \frac{k_i k_j}{N \langle k \rangle} \quad (4.2)$$

, in addition assuming inhomogeneous external field $h \rightarrow k_i h$.

A sum of any function of the degrees over all nodes can be expressed as

$$\frac{1}{N} \sum_i f(k_i) = \sum_{k=k_{\min}}^{k_{\max}} P(k) f(k). \quad (4.3)$$

In the infinite network limit $N \rightarrow \infty$, $k_{\max} \rightarrow \infty$, we can change the summation into an integration. Then we can calculate the free energy of the

AT model on uncorrelated scale-free networks:

$$g = \beta F/N$$

$$\begin{aligned}
& \simeq -\frac{1}{N} \sum_i \ln \left[\cosh \left(\sum_{j(i)} K_2 \frac{k_i k_j}{N \langle k \rangle} m_s^j + k_i h_s \right) \cosh \left(\sum_{j(i)} K_2 \frac{k_i k_j}{N \langle k \rangle} m_\sigma^j + k_i h_\sigma \right) \right. \\
& \quad \times \cosh \left(\sum_{j(i)} K_4 \frac{k_i k_j}{N \langle k \rangle} m_{s\sigma}^j + k_i h_{s\sigma} \right) + \sinh \left(\sum_{j(i)} K_2 \frac{k_i k_j}{N \langle k \rangle} m_s^j + k_i h_s \right) \\
& \quad \times \sinh \left(\sum_{j(i)} K_2 \frac{k_i k_j}{N \langle k \rangle} m_\sigma^j + k_i h_\sigma \right) \sinh \left(\sum_{j(i)} K_4 \frac{k_i k_j}{N \langle k \rangle} m_{s\sigma}^j + k_i h_{s\sigma} \right) \left. \right] \\
& + \frac{1}{2N} \sum_{i,j} K_2 \frac{k_i k_j}{N \langle k \rangle} m_s^i m_s^j + \frac{1}{2N} \sum_{i,j} K_2 \frac{k_i k_j}{N \langle k \rangle} m_\sigma^i m_\sigma^j + \frac{1}{2N} \sum_{i,j} K_4 \frac{k_i k_j}{N \langle k \rangle} m_{s\sigma}^i m_{s\sigma}^j \\
& \simeq - \int_{k_{\min}}^{\infty} \ln \left[\cosh (K_2 m_s k + k h_s) \cosh (K_2 m_\sigma k + k h_\sigma) \cosh (K_4 m_{s\sigma} k + k h_{s\sigma}) \right. \\
& \quad \left. + \sinh (K_2 m_s k + k h_s) \sinh (K_2 m_\sigma k + k h_\sigma) \sinh (K_4 m_{s\sigma} k + k h_{s\sigma}) \right] P(k) dk \\
& + \frac{1}{2} K_2 m_s^2 \langle k \rangle + \frac{1}{2} K_2 m_\sigma^2 \langle k \rangle + \frac{1}{2} K_4 m_{s\sigma}^2 \langle k \rangle \tag{4.4}
\end{aligned}$$

This mean free energy serves as a significant cornerstone in obtaining a great diversity of thermodynamic quantities.

4.2 Equations of state

The magnetizations of each spin is obtained from the partial derivative of the free energy with respect to the external field and then taking the zero-field

limit. Noting that $h \rightarrow k_i h$ from Eq. (3.3), we can find the following result,

$$\begin{aligned}
\left. \frac{\partial g}{\partial h_s} \right|_{h=0} &= \left. \frac{\beta}{N} \frac{\partial F}{\partial h_s} \right|_{h=0} = - \left. \frac{\beta}{N} \frac{\partial \left(\frac{1}{\beta} \ln Z \right)}{\partial h_s} \right|_{h=0} = - \left. \frac{1}{N} \frac{1}{Z} \frac{\partial Z}{\partial h_s} \right|_{h=0} \\
&= - \frac{1}{N} \frac{1}{\sum_{all \text{ config.}} e^{-\beta \mathcal{H}}} \frac{\partial}{\partial h_s} \left(\sum_{all \text{ config.}} e^{-\beta \mathcal{H}} \right) \Big|_{h=0} \\
&= - \frac{1}{N} \frac{\sum_{all \text{ config.}} \left(\sum_i k_i s_i e^{-\beta \mathcal{H}} \right)}{\sum_{all \text{ config.}} e^{-\beta \mathcal{H}}} \\
&\simeq - \frac{1}{N} \langle \sum_i k_i m_s^i \rangle_B = - \frac{1}{N} \langle m_s \sum_i k_i \rangle_B = - \frac{1}{N} \langle m_s N \langle k \rangle \rangle_B \\
&= - m_s \langle k \rangle.
\end{aligned} \tag{4.5}$$

Likewise, similar relations for other spins are given by

$$\left. \frac{\partial g}{\partial h_\sigma} \right|_{h=0} \simeq - m_\sigma \langle k \rangle \tag{4.6}$$

$$\left. \frac{\partial g}{\partial h_{s\sigma}} \right|_{h=0} \simeq - m_{s\sigma} \langle k \rangle. \tag{4.7}$$

This time, we will calculate these partial derivatives using the annealed mean field free energy already obtained in the infinite network limit:

$$\begin{aligned}
\left. \frac{\partial g}{\partial h_s} \right|_{h=0} &\simeq - \int_{k_{\min}}^{\infty} \left[k \sinh(K_2 m_s k) \cosh(K_2 m_\sigma k) \cosh(K_4 m_{s\sigma} k) \right. \\
&\quad \left. + k \cosh(K_2 m_s k) \sinh(K_2 m_\sigma k) \sinh(K_4 m_{s\sigma} k) \right] \\
&\quad \Big/ \left[\cosh(K_2 m_s k) \cosh(K_2 m_\sigma k) \cosh(K_4 m_{s\sigma} k) \right. \\
&\quad \left. + \sinh(K_2 m_s k) \sinh(K_2 m_\sigma k) \sinh(K_4 m_{s\sigma} k) \right] P(k) dk \\
&= - \int_{k_{\min}}^{\infty} \left[\frac{\tanh(K_2 m_s k) + \tanh(K_2 m_\sigma k) \tanh(K_4 m_{s\sigma} k)}{1 + \tanh(K_2 m_s k) \tanh(K_2 m_\sigma k) \tanh(K_4 m_{s\sigma} k)} \right] k P(k) dk.
\end{aligned} \tag{4.8}$$

Likewise,

$$\left. \frac{\partial g}{\partial h_\sigma} \right|_{h=0} \simeq - \int_{k_{\min}}^{\infty} \left[\frac{\tanh(K_2 m_\sigma k) + \tanh(K_2 m_s k) \tanh(K_4 m_{s\sigma} k)}{1 + \tanh(K_2 m_s k) \tanh(K_2 m_\sigma k) \tanh(K_4 m_{s\sigma} k)} \right] k P(k) dk \quad (4.9)$$

$$\left. \frac{\partial g}{\partial h_{s\sigma}} \right|_{h=0} \simeq - \int_{k_{\min}}^{\infty} \left[\frac{\tanh(K_4 m_{s\sigma} k) + \tanh(K_2 m_s k) \tanh(K_2 m_\sigma k)}{1 + \tanh(K_2 m_s k) \tanh(K_2 m_\sigma k) \tanh(K_4 m_{s\sigma} k)} \right] k P(k) dk \quad (4.10)$$

Finally, we obtain the equations of the state from 4.8), (4.9), (4.10), (4.5), (4.6), (4.7)

$$m_s \langle k \rangle \simeq \int_{k_{\min}}^{\infty} \left[\frac{\tanh(K_2 m_s k) + \tanh(K_2 m_\sigma k) \tanh(K_4 m_{s\sigma} k)}{1 + \tanh(K_2 m_s k) \tanh(K_2 m_\sigma k) \tanh(K_4 m_{s\sigma} k)} \right] k P(k) dk \quad (4.11)$$

$$m_\sigma \langle k \rangle \simeq \int_{k_{\min}}^{\infty} \left[\frac{\tanh(K_2 m_\sigma k) + \tanh(K_2 m_s k) \tanh(K_4 m_{s\sigma} k)}{1 + \tanh(K_2 m_s k) \tanh(K_2 m_\sigma k) \tanh(K_4 m_{s\sigma} k)} \right] k P(k) dk \quad (4.12)$$

$$m_{s\sigma} \langle k \rangle \simeq \int_{k_{\min}}^{\infty} \left[\frac{\tanh(K_4 m_{s\sigma} k) + \tanh(K_2 m_s k) \tanh(K_2 m_\sigma k)}{1 + \tanh(K_2 m_s k) \tanh(K_2 m_\sigma k) \tanh(K_4 m_{s\sigma} k)} \right] k P(k) dk. \quad (4.13)$$

The equations of state can also found using the minimization conditions of free energy, that is, differentiating with respect to each order parameter and then equating this to 0. One can find several solutions that satisfy these equations of state. Out of these, we only select the solutions that are thermodynamically stable, i.e., minimize the mean field free energy Eq. (4.4). The other unstable or metastable solutions can be discarded.

4.3 Example 1 : the Ising model

The AT model becomes two-independent Ising models at the decoupling point $K_4 = 0$, which means that four-spin interaction disappears. For the sake of simplicity, we choose a homogeneous space, i.e., $P(k) = \delta(k - k_0)$. Then, the equation of state for s -spin is given by

$$\begin{aligned}
m_s \langle k \rangle &\simeq \int_{k_{\min}}^{\infty} \left[\frac{\tanh(K_2 m_s k) + \tanh(K_2 m_\sigma k) \tanh(K_4 m_{s\sigma} k)}{1 + \tanh(K_2 m_s k) \tanh(K_2 m_\sigma k) \tanh(K_4 m_{s\sigma} k)} \right] k P(k) dk \\
&= \int_{k_{\min}}^{\infty} [\tanh(K_2 m_s k)] k \delta(k - k_0) dk \\
m_s k_0 &\simeq \tanh(K_2 m_s k_0) k_0 \\
m_s &\simeq \tanh(K_2 m_s k_0)
\end{aligned} \tag{4.14}$$

This result is the well-known equation of state for the Ising model in the standard mean field approximation. Hence we can see that we're on the right track.

4.4 Example 2 : the 4-state Potts model

When $K_4 = K_2$ ($m_s = m_\sigma = m_{s\sigma}$), the isotropic AT model can be reduced to the four-state Potts model. As mentioned earlier, the q -state Potts model on complex networks has been studied deeply, using a variety of methods. Given q -state on scale-free networks, it is known that the critical degree exponents which lies on the marginal line divide the regions of first- and second-order phase transition. At $q = 4$, the value of the critical degree exponent λ_c is about 3.5 [29, 30].

Now, we deal with this isotropic AT model ($K_2 = K_4$). It's universality class is equivalent to that of the four-state Potts model. Because of this symmetry, the three degrees of freedom of the order parameters collapse to one. Thus, we can

rewrite the annealed mean field free energy Eq. (4.4) and the self-consistency equation Eqs. (4.11) to (4.13) as

$$g_{\text{potts}} \simeq - \int_{k_{\min}}^{\infty} \ln \left[\left(\cosh (K_2 m_p k + k h_p) \right)^3 + \left(\sinh (K_2 m_p k + k h_p) \right)^3 \right] P(k) dk + \frac{3}{2} K_2 m_p^2 \langle k \rangle \quad (4.15)$$

and

$$m_p \langle k \rangle \simeq \int_{k_{\min}}^{\infty} \left[\frac{\tanh (K_2 m_p k) + \left(\tanh (K_2 m_p k) \right)^2}{1 + \left(\tanh (K_2 m_p k) \right)^3} \right] k P(k) dk. \quad (4.16)$$

Noting that

$$\ln[(\cosh[x])^3 + (\sinh[x])^3] \simeq \frac{3}{2}x^2 + x^3 - \frac{1}{4}x^4 - x^5 - \frac{13}{30}x^6 + \frac{11}{15}x^7 + \frac{823}{840}x^8 + \dots, \quad (4.17)$$

we can extract the divergent term for $3 < \lambda < 4$ in the integrand of Eq. (4.15).

$$g_{\text{potts}} \simeq -\frac{3}{2} K_2^2 m_p^2 \langle k^2 \rangle + \frac{3}{2} K_2 m_p^2 \langle k \rangle + \int_{k_{\min}}^{\infty} \phi[K_2 m_p k] P(k) dk \quad (4.18)$$

where

$$\phi[x] \simeq -\ln \left[(\cosh(x))^3 + (\sinh(x))^3 \right] + \frac{3}{2}x^2. \quad (4.19)$$

Setting $P(k) = N_\lambda k^{-\lambda}$, the free energy is given by

$$g_{\text{potts}} \simeq \frac{3}{2} K_2 m_p^2 \langle k \rangle \left(1 - \frac{K_2 \langle k^2 \rangle}{\langle k \rangle} \right) + N_\lambda (K_2 m_p)^{\lambda-1} C_\lambda^p \quad (4.20)$$

where

$$C_\lambda^p \equiv \int_{x_{\min}}^{\infty} \phi[x] x^{-\lambda} dx \quad (4.21)$$

with $x_{\min} = K_2 m_p k_{\min}$.

For $x_{min} \rightarrow 0$, C_λ^p has a finite real value. In spirit of the Landau theory, a continuous and discontinuous phase transition emerge for $C_\lambda^p > 0$ and $C_\lambda^p < 0$, respectively. Of course, the sign of the next order order parameter which is larger than $O(m^{\lambda-1})$, is always positive. Then, the critical degree exponent must be located at $C_{\lambda_c}^p = 0$. After some numerical calculations, we obtain the value of the critical degree exponent to be 3.5034. This value closely resembles that obtained by Iglói *etal.* and M. Krasnytska *et al.* [29, 30].

Next, let us find the magnetization in the vicinity of the critical temperature for the region of the second-order phase transition. Setting $T_0 \equiv \frac{J_2 \langle k^2 \rangle}{\langle k \rangle}$, we consider the minimum of the free energy with respect to the magnetization. For $T > T_0$, the free energy is minimized when the magnetization is zero. For $T < T_0$, there is a non-zero magnetization that minimizes the free energy. In order to find this, we equate the partial derivative of the free energy with respect to the magnetization with 0.

$$\frac{\partial g_{\text{potts}}}{\partial m_p} \simeq 3K_2 m_p \langle k \rangle \left(1 - \frac{T_0}{T} \right) + N_\lambda (\lambda - 1) K_2 (K_2 m_p)^{\lambda-2} C_\lambda^p = 0. \quad (4.22)$$

Near the critical point $T \simeq T_0^-$, the magnetization is given by

$$m_p \simeq T^{\frac{\lambda-2}{\lambda-3}} \left(\frac{3J_2^{2-\lambda} \langle k \rangle}{N_\lambda (\lambda - 1) C_\lambda^p} \tau \right)^{\frac{1}{\lambda-3}} = T^{\frac{\lambda-2}{\lambda-3}} (C'_\lambda \tau)^{\frac{1}{\lambda-3}} \quad (4.23)$$

where $C'_\lambda \equiv \frac{3J_2^{2-\lambda} \langle k \rangle}{N_\lambda (\lambda - 1) C_\lambda^p}$ and $\tau \equiv \frac{T - T_0}{T_0}$. This means that the critical exponent $\beta = \frac{1}{\lambda-3}$ for $3 < \lambda_c < 4$. Also, It is the same β which Iglói *et al.* and M. Krasnytska *etal.* mentioned [29, 30].

4.5 Critical degree exponent of the AT model

In the previous section, we found the critical degree exponent corresponding to the four-state Potts model with $x = \frac{K_4}{K_2} = 1$. Then, what will its value be for

$x > 0$ and $x \neq 1$? Is it larger than or less than λ_c^p at $x = 1$? Or, is it the same as λ_c^p ? Whichever conclusion we come to, it is a crucial issue that both the degree exponent λ and the ratio of coupling strengths $x = \frac{K_4}{K_2}$ determine the type of phase transition. To see this, let us start from the free energy Eq. (4.4) given by

$$\begin{aligned}
g \simeq & - \int_{k_{\min}}^{\infty} \ln [\cosh (K_2 m_s k) \cosh (K_2 m_{\sigma} k) \cosh (K_4 m_{s\sigma} k) \\
& + \sinh (K_2 m_s k) \sinh (K_2 m_{\sigma} k) \sinh (K_4 m_{s\sigma} k)] P(k) dk \\
& + \frac{1}{2} K_2 m_s^2 \langle k \rangle + \frac{1}{2} K_2 m_{\sigma}^2 \langle k \rangle + \frac{1}{2} K_4 m_{s\sigma}^2 \langle k \rangle + m_s \langle k \rangle h_s + m_{\sigma} \langle k \rangle h_{\sigma} + m_{s\sigma} \langle k \rangle h_{s\sigma}.
\end{aligned} \tag{4.24}$$

For $x > 0$, the three degrees of freedom of the order parameters is reduced to two due to the symmetry of the magnetizations m_s , m_{σ} . If we write $m \equiv m_s = m_{\sigma}$ and $M \equiv m_{s\sigma}$, the free energy Eq. (4.24) will be expressed as

$$\begin{aligned}
g \simeq & + K_2 m^2 \langle k \rangle + \frac{1}{2} K_4 M^2 \langle k \rangle + 2m \langle k \rangle h_s + M \langle k \rangle h_{s\sigma} \\
& - \int_{k_{\min}}^{\infty} \ln [(\cosh (K_2 m k))^2 \cosh (K_4 M k) \\
& + (\sinh (K_2 m k))^2 \sinh (K_4 M k)] P(k) dk \\
\simeq & + K_2 m^2 \langle k \rangle + \frac{1}{2} K_4 M^2 \langle k \rangle + 2m \langle k \rangle h_s + M \langle k \rangle h_{s\sigma} \\
& - 2 \int_{k_{\min}}^{\infty} \ln [\cosh (K_2 m k)] P(k) dk - \int_{k_{\min}}^{\infty} \ln [\cosh (K_4 M k)] P(k) dk \\
& - \int_{k_{\min}}^{\infty} \ln [1 + (\tanh (K_2 m k))^2 \tanh (K_4 M k)] P(k) dk.
\end{aligned} \tag{4.25}$$

In the same way as we have done in the previous section, we restrict the

degree exponent to $3 < \lambda < 4$ and extract the divergent part in the integrand:

$$\begin{aligned}
g \simeq & +K_2 m^2 \langle k \rangle + \frac{1}{2} K_4 M^2 \langle k \rangle + 2m \langle k \rangle h_s + M \langle k \rangle h_{s\sigma} \\
& 2N_\lambda (K_2 m)^\lambda C_m[\lambda] - K_2^2 m^2 \langle k^2 \rangle + N_\lambda (K_4 M)^\lambda C_M[\lambda] - \frac{1}{2} K_4^2 M^2 \langle k^2 \rangle \\
& - \int_{k_{\min}}^{\infty} \ln \left[1 + (\tanh(K_2 m k))^2 \tanh(K_4 M k) \right] P(k) dk
\end{aligned} \tag{4.26}$$

where

$$C_m[\lambda] = C_M[\lambda] \equiv - \int_{x_{\min}}^{\infty} \left(\ln[\cosh(x)] - \frac{1}{2} x^2 \right) P(x) dx. \tag{4.27}$$

We define the function including the coupled order parameters as

$$g_{\text{couple}} \equiv \int_{k_{\min}}^{\infty} G_{\text{couple}}[mk, Mk] P(k) dk \tag{4.28}$$

where

$$G_{\text{couple}}[mk, Mk] \simeq - \ln \left[1 + (\tanh(K_2 m k))^2 \tanh(K_4 M k) \right]. \tag{4.29}$$

Considering the symmetric form of $G_{\text{couple}}[mk, Mk]$, we construct an ansatz:

$$g_{\text{couple}} \equiv C_{\text{couple}}[\lambda] (K_2^2 K_4 m^2 M)^{\frac{\lambda-1}{3}} \tag{4.30}$$

where

$$C_{\text{couple}}[\lambda] \simeq - \int_{x_{\min}}^{\infty} \ln \left[1 + (\tanh(x))^3 \right] P(x) dx. \tag{4.31}$$

Finally, we obtain the following mean field free energy which consists of the two order parameters for $3 < \lambda < 4$:

$$\begin{aligned}
g \simeq & +K_2 m^2 \langle k \rangle + \frac{1}{2} K_4 M^2 \langle k \rangle + 2m \langle k \rangle h_s + M \langle k \rangle h_{s\sigma} \\
& - K_2^2 m^2 \langle k^2 \rangle - \frac{1}{2} K_4^2 M^2 \langle k^2 \rangle \\
& + 2N_\lambda C_m[\lambda] (K_2 m)^\lambda + N_\lambda C_M[\lambda] (K_4 M)^\lambda + N_\lambda C_{\text{couple}}[\lambda] (K_2^2 K_4 m^2 M)^{\frac{\lambda-1}{3}}.
\end{aligned} \tag{4.32}$$

We can make an approximation $M \simeq am$ in the first-order phase transition, because the orders of magnetizations M and m are linear. Using $C_m[\lambda] = C_M[\lambda]$ and $x = J_4/J_2$, the mean field free energy is given by

$$\begin{aligned}
g &\simeq +K_2 m^2 \langle k \rangle + \frac{1}{2} K_4 a^2 m^2 \langle k \rangle + 2m \langle k \rangle h_s + am \langle k \rangle h_{s\sigma} \\
&\quad - K_2^2 m^2 \langle k^2 \rangle - \frac{1}{2} K_4^2 a^2 m^2 \langle k^2 \rangle \\
&\quad + 2N_\lambda C_m[\lambda] (K_2 m)^{\lambda-1} + N_\lambda C_m[\lambda] (K_4 am)^{\lambda-1} + N_\lambda C_{\text{couple}}[\lambda] (K_2^2 K_4 am^3)^{\frac{\lambda-1}{3}} \\
&\simeq +2m \langle k \rangle h_s + am \langle k \rangle h_{s\sigma} \\
&\quad + \left(K_2 \langle k \rangle - K_2^2 \langle k^2 \rangle + \frac{1}{2} \left(K_4 \langle k \rangle - K_4^2 \langle k^2 \rangle \right) a^2 \right) m^2 \\
&\quad + N_\lambda K_2^{\lambda-1} \left(2C_m[\lambda] + C_m[\lambda] (xa)^{\lambda-1} + C_{\text{couple}}[\lambda] (xa)^{\frac{\lambda-1}{3}} \right) m^{\lambda-1}. \tag{4.33}
\end{aligned}$$

Let us define the terms in the parenthesis of the last term to be:

$$C_{\text{part}} \equiv 2C_m[\lambda] + C_m[\lambda] (xa)^{\lambda-1} + C_{\text{couple}}[\lambda] (xa)^{\frac{\lambda-1}{3}}. \tag{4.34}$$

Trivially for $x < 1$, m is larger than M which means $ax < 1$. For $x > 1$, m is less than M which means $ax > 1$. Now, we just focus on how the sign of C_{part} changes depending on x , keeping $a = 1$ fixed. This is only possible near the Potts point ($x = 1$). Then, C_{part} becomes,

$$C_{\text{part}}[x, \lambda] \simeq 2C_m[\lambda] + C_m[\lambda] (x)^{\lambda-1} + C_{\text{couple}}[\lambda] (x)^{\frac{\lambda-1}{3}}. \tag{4.35}$$

The critical degree exponent must be located at $C_{\text{part}}[x, \lambda_c] = 0$. It is clear that the sign of the next order order parameter, is always positive. After some numerical calculations, we obtain the critical degree exponent as a function of x in the vicinity of the Potts point. If we plot the dependence of $C_{\text{part}}[x, \lambda_c]$ on x , we obtain a convex line (Fig. 4.1). The area above(below) this line is characterized by first-order(second-order) phase transition. This phase diagram shows that the Potts point at the isotropic AT model on uncorrelated scale-free networks is the minimum value of the critical degree exponent.

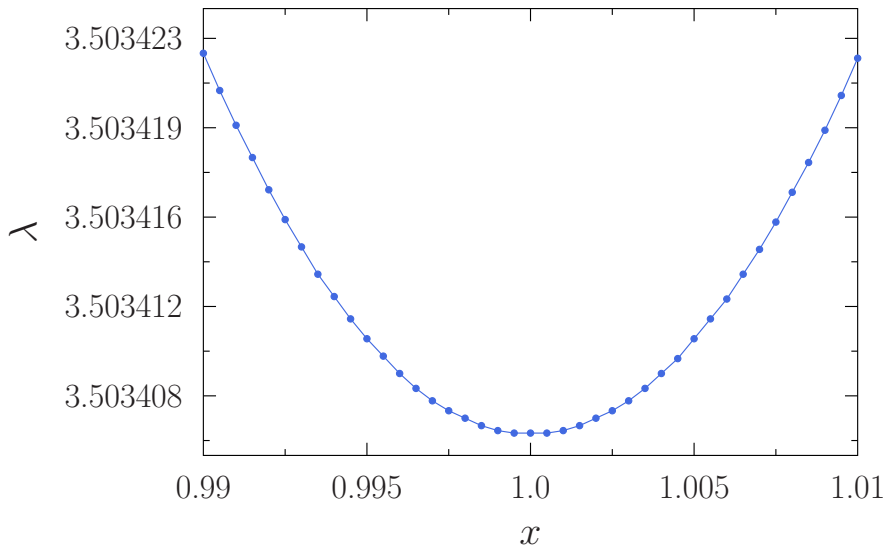


Figure 4.1 The phase diagram of the isotropic AT model on uncorrelated scale-free networks. λ is the degree exponent and x is the ratio of the coupling strengths (J_4/J_2). Blue points indicate the critical degree exponents obtained by numerical calculation. The regime over the line belongs to the first-order phase transition, while that below belongs to the second-order phase transition. The Potts point is at $x = 1$, which is equivalent to universality class of the 4-state Potts model. The Potts point is the minimum of λ . This implies that system on the Potts point($x = 1$) need stronger hubs to change type of ordering from first-order to second-order transition.

4.6 Brief simulation results

We investigate the order parameters, that is, the magnetizations, $\langle \sigma \rangle$, $\langle s \rangle$, $\langle \sigma s \rangle$, and $\langle \sigma s \rangle_{AF}$, matching them to the red, green, blue, and purple points, respectively in Fig. 4.2~Fig. 4.9.

For $x = 1$, we confirmed that the isotropic AT model is exactly the same

with the 4-state Potts model which is equivalent to $\langle\sigma\rangle = \langle s\rangle = \langle\sigma s\rangle$ in Fig. 4.2. In the case of $x = 0$, the AT model maps into the independent Ising model trivially (see Fig. 4.3). Surprisingly, for $x \leq -1$, the $\langle\sigma\rangle$ phase occurs suddenly near $x \sim -1$, as in Fig. 4.4~Fig. 4.9. This phase never appears for $x > -1$. Even if x goes over -1 , the $\langle\sigma s\rangle_{AF}$ phase is never dominant. Moreover, $\langle\sigma\rangle$ phase never disappears for $x < -1$. These results on scale-free networks are very different from those on square lattice or Cayley tree. Thus, we conjecture that there are coexistence phases of $\langle\sigma s\rangle_{AF}$ (but weak) and $\langle\sigma\rangle$ for $x < -1$.

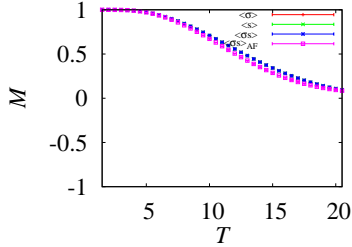


Figure 4.2 Magnetizations of the AT model on scale-free networks depending on temperature($T, k_B = 1$) with $\lambda = 3.6$, N (the number of nodes)= 50000, and $x = 1.0$

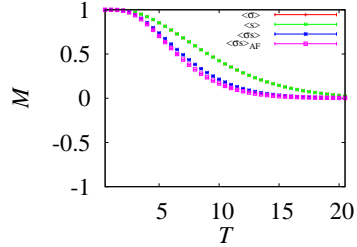


Figure 4.3 Magnetizations of the AT model on scale-free networks depending on temperature($T, k_B = 1$) with $\lambda = 3.6$, N (the number of nodes)= 50000, and $x = 0.0$

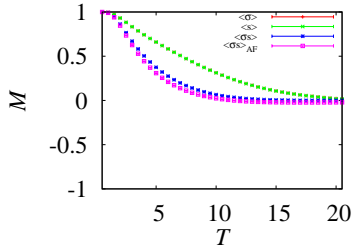


Figure 4.4 Magnetizations of the AT model on scale-free networks depending on temperature($T, k_B = 1$) with $\lambda = 3.6$, N (the number of nodes)= 50000, and $x = -0.5$

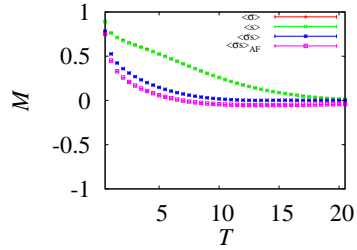


Figure 4.5 Magnetizations of the AT model on scale-free networks depending on temperature($T, k_B = 1$) with $\lambda = 3.6$, N (the number of nodes)= 50000, and $x = -0.9$

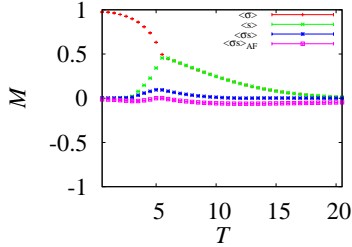


Figure 4.6 Magnetizations of the AT model on scale-free networks depending on temperature($T, k_B = 1$) with $\lambda = 3.6$, N (the number of nodes)= 50000, and $x = -1.0$

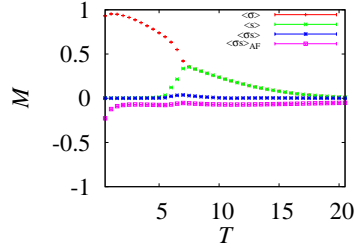


Figure 4.7 Magnetizations of the AT model on scale-free networks depending on temperature($T, k_B = 1$) with $\lambda = 3.6$, N (the number of nodes)= 50000, and $x = -1.1$

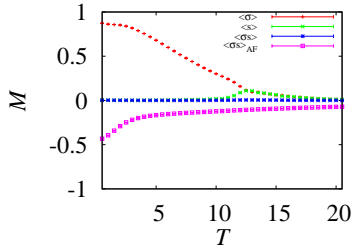


Figure 4.8 Magnetizations of the AT model on scale-free networks depending on temperature($T, k_B = 1$) with $\lambda = 3.6$, N (the number of nodes)= 50000, and $x = -1.5$

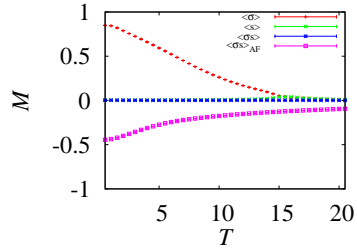


Figure 4.9 Magnetizations of the AT model on scale-free networks depending on temperature($T, k_B = 1$) with $\lambda = 3.6$, N (the number of nodes)= 50000, and $x = -2.0$

Chapter 5

Conclusion

We have looked around the historical background of the AT model on a variety of structures such as the square lattice and the Bethe lattice(Cayley tree). It is sufficiently worth studying the AT model because it has a richness of phases and critical transition phenomena due to the competitions between coupling strengths and the characteristics of the structure. Unfortunately, to acquire the exact solution of the anisotropic($J_{2,s} \neq J_{2,\sigma}$) AT model is difficult, especially on uncorrelated scale-free networks. Thus, techniques such as high- and low- temperature series, Monte Carlo simulations, mean-field calculations, and renormalization group are essential to analyzing the behavior of the AT model on the diverse systemic structures.

We restricted the our case to the isotropic($J_{2,s} = J_{2,\sigma}$) AT model on uncorrelated scale-free networks, are considered only the ferromagnetic regime, i.e., $x > 0$ for the analytic solution. In spirit of the Landau theory and mean field theory, we obtained approximately the critical degree exponent $\lambda_c^p = 3.5034$ at the Potts point($x = 1$) which is equivalent to the universality class of the 4-state

Potts model. Furthermore, using several assumptions, we conjectured that the value of the critical degree exponent will become larger as the distance from $x = 1$ increases in the ferromagnetic regime. In other words, the Potts point at the isotropic AT model on uncorrelated scale-free networks is the minimum value of the critical degree exponents and first-order phase transition can exist even for the fat-tailed degree distribution. Also, it implies that the system with lower values of the critical degree exponent requires stronger hubs to change from first-order to second-order transition. The spins remain ordered at any finite temperatures as long as the value of λ is less than 3. Second-order phase transition dominates the whole range of x in the interval $3 < \lambda < \lambda_c^p$. At $\lambda = \lambda_c^p$, first transition emerges at the Potts point($x = 1$). As the degree exponent become larger, the regime of the first-order phase transition with respect to x spreads out from $x = 1$ to the range of x obtained by the standard mean-field approximation in the Erdős-Rényi limit.

Moreover, we performed the Monte-Carlo simulations for several ranges of x and investigated the order parameters to sketch the phase diagram. We discovered, in this diagram, that the anti-ferromagnetic phase $\langle \sigma s \rangle_{AF}$ cannot exist. Also, the range of x for where the $\langle \sigma \rangle$ phase emerges on scale-free networks are very different from that on the periodic lattice or the tree-like structure. That is, for $x < -1$, the $\langle \sigma \rangle$ phase is mixed up with the $\langle \sigma s \rangle_{AF}$ phase. The reason is that scale-free networks generally have the geometrical structure on which we inevitably encounter frustration. Meanwhile, we expect that if $J_4/J > 0$, the whole outline of the shape of the AT model's phase diagram on scale-free networks would be analogous to that on the Bethe lattice(Cayley tree), because the scale-free network possesses an intrinsic tree-like local structure.

In the near future, we might be able solve the AT model on networks by other analytic approaches, assuming that networks basically have tree-like structures.

On the basis of these knowledge, we could explain the diverse collective critical phenomena reflecting the AT model on the scale-free networks such as the Ising model on networks with an arbitrary distribution, which was already studied by Dorogovtsev [26].

Bibliography

- [1] S. V. Buldyrev, R. Parshani, G. Paul, H. E. Stanley, and S. Havlin, *Nature* **464**, 1025 (2010).
- [2] A.-L. Barabási and R. Albert, *Science* **286**, 509 (1999).
- [3] R. Albert and A.-L. Barabási, *Rev. Mod. Phys.* **74**, 47 (2002).
- [4] K. Suchecki and J. A. Holyst, *Phys. Rev. E* **74**, 011122 (2006).
- [5] K. Suchecki and J. A. Holyst, *Phys. Rev. E* **80**, 031110 (2009).
- [6] J. Ashkin and E. Teller, *Phys. Rev.* **64**, 178 (1943).
- [7] R. V. Ditzian, J. R. Banavar, G. S. Grest, and L. P. Kadanoff, *Phys. Rev. B* **22**, 2542 (1980).
- [8] C. Fan, *Phys. Lett. A* **39**, 136 (1972).
- [9] F. J. Wegner, *J. Phys. C* **5**, L131 (1972).
- [10] J. Chahine, J. R. D. de Felicio, and N. Caticha, *J. Phys. A: Math. Gen.* **22**, 1639 (1989).
- [11] S. Wiseman and E. Domany, *Phys. Rev. E* **51**, 3074 (1995).

- [12] G. Kamieniarz, P. Kozłowski, and R. Dekeyser, Phys. Rev. E **55**, 3724 (1997).
- [13] P. Bak, P. Kleban, W. N. Unertl, J. Ochab, G. Akinici, N. C. Bartelt, and T. L. Einstein, Phys. Rev. Lett. **54**, 1539 (1985).
- [14] L. P. Kadanoff, Phys. Rev. Lett. **39**, 903 (1977).
- [15] H. Knops, Ann. Phys. **128**, 448 (1980).
- [16] M. P. M. den Nijs, Phys. Rev. B **23**, 6111 (1981).
- [17] J. A. Plascak and F. C. S. Barreto, J. Phys. A: Math. Gen. **19**, 2195 (1986).
- [18] P. Arnold, Nucl. Phys. B **501**, 803 (1997).
- [19] G. Musiał, L. Dębski, and G. Kamieniarz, Phys. Rev. B **66**, 012407 (2002).
- [20] G. Musiał, Phys. Rev. B **69**, 024407 (2004).
- [21] J. M. de Araujo and F. A. da Costa, Braz. J. Phys. **27**, 89 (1997).
- [22] L. Jian-Xin and Y. Zhan-Ru, Commun. Theor. Phys. **43**, 841 (2005).
- [23] A. Aleksiejuk, J. Holyst, and D. Stauffer, Phys. A **310**, 260 (2002).
- [24] G. Bianconi, Phys. Lett. A **303**, 166 (2002).
- [25] M. Leone, A. Vázquez, A. Vespignani, and R. Zecchina, Eur. Phys. J. B **28**, 191 (2002).
- [26] S. N. Dorogovtsev, A. V. Goltsev, and J. F. F. Mendes, Phys. Rev. E **66**, 016104 (2002).
- [27] S. H. Lee, M. Ha, H. Jeong, J. D. Noh, and H. Park, Phys. Rev. E **80**, 051127 (2009).

- [28] S. Dorogovtsev, A. Goltsev, and J. Mendes, Eur. Phys. J. B **38**, 177 (2004).
- [29] F. Iglói and L. Turban, Phys. Rev. E **66**, 036140 (2002).
- [30] M. Krasnytska, B. Berche, and Y. Holovatch, Condens. Matter phys. **16**, 23602 (2013).

요약

복잡계 네트워크 상에서의 다양한 스핀모형에 대한 연구는 자연현상에서 집단 떠오름 현상을 이해하는데 아주 중요한 역할을 한다. 이에 따라 지난 10년간 네트워크 상에서의 이징 모형과 팻츠 모형이 주목을 받아 왔다. 대다수의 실제 세상의 네트워크는 네트워크들의 네트워크 구조로 이루어져 있기 때문에 근래에 들어 다층 구조의 네트워크에서의 연구가 활발하게 진행되고 있다. 그럼에도 불구하고 네트워크 내부 및 네트워크 간의 상호작용을 고려하여 기술하는 스핀모형을 연구는 극히 드물다.

이러한 일환으로 우리는 척도 없는 임의의 네트워크 상에서의 에쉬킨-텔러 모형을 연구하였다. 에쉬킨-텔러 모형에서 각 지점에서의 스핀들은 두가지 종류의 스핀으로 이루어져 있으며, 각각의 스핀들은 가장 인접한 이웃의 같은 종류의 스핀들과 J_2 의 짝힘의 세기로 상호작용을 하고, 서로 다른 두 종류의 스핀들은 네가지 스핀이 고려되어 J_4 의 짝힘의 세기로 상호작용을 한다. 다시 말하자면, 짝힘의 세기 J_2 는 각 내부 네트워크에서의 상호작용에 대응되며, 짝힘의 세기 J_4 는 네트워크 간의 상호작용에 대응된다.

짝힘의 세기 비율 $x = J_4/J_2$ 에 의존하여, 다양한 상들이 떠오를 수 있다. 이는 이미 평균장 근사를 통하여 이전에 얻어졌던 결과로, 각 상의 종류에는 상자성의 상, 강자성의 상, 반강자성의 상, 벡스터 상, 시그마 상이 있을 수 있다. 우리는 평균장 풀이로 얻어진 상그림과 척도 없는 네트워크에서의 상그림을 비교, 분석할 것이다. 상자성의 상과 벡스터 상 간의 상전이는 평균장 이론에 따르면 불연속임에 반하여, 척도 없는 네트워크에서는 도수 지수에 따라 연속 상전이가 될 수 있다. 란다우 이론에 입각하여, 우리는 1차 상전이와 2차 상전이의 영역이 나누어지는 경계선에 초점을 맞출 것이며, 해석적인 접근 방식으로 부여된 짝힘의 세기의 비율 x 에 관하여 임계 도수 지수를 얻을 것이다.

이에 더하여, 우리는 $x < 0$ 부분에 한하여 개략적인 상그림을 예측하기 위하여 몬테카를로 방법을 확장할 것이다. 메트로폴리스 알고리즘을 이용하여 우리는 시뮬레이션을 수행하였으며, 자화, 열용량, 민감도, 빈터큐물런트와 같은 다양한 열역학적 양들을 얻는다. x 가 임수인 영역에서 찢찢뿔뿔현상으로 인하여 변칙적인 양상이 관측될 수 있다.

마지막으로 우리는 해석적인 결과와 시뮬레이션의 결과를 고려할 것이며, 평균장 수준에서 균질한 공간에서와 비균질한 척도 없는 네트워크 상에서의 차이에 대하여 내포된 의미를 토론할 것이다.

주요어: 에쉬킨-텔러 모형, 척도 없는 네트워크, 연속 상전이, 불연속 상전이, 임계 도수 지수, 삼중 임계점, 몬테-카를로 방법, 메트로폴리스 알고리즘
학번: 2012-22512